F. K. Lamb and P. Ghosh

Interaction of Accretion Disks with Magnetospheres

ABSTRACT. Disk-magnetosphere interaction strongly affects the observable properties of magnetic compact stars accreting from disks. This article reviews some of the physical processes that are thought to be important in low-mass binary systems containing weakly magnetic neutron stars. We summarize recent work on the interaction of the inner disk with the stellar magnetic field in such systems and on a unified model of their X-ray spectral states and quasi-periodic intensity oscillations. Finally, magnetospheric mechanisms are described that may accelerate particles to GeV or even TeV energies.

1. INTRODUCTION

Interaction of the inner part of the accretion disk with the magnetic field of the star plays an important role in determining the observable properties of compact stars accreting from disks. This article reviews some of the physical processes that are thought to be important in low-mass X-ray binaries (LMXBs) containing weakly magnetic accreting neutron stars. These processes include electrodynamic interaction of the disk plasma with the stellar magnetic field, termination of the Keplerian disk flow by magnetic stresses, creation of a compact central corona surrounding the magnetosphere, Comptonization of radiation produced near the neutron star, and acceleration of charged particles to high energies.

In §2 we summarize recent work on the interaction of the inner disk with the stellar magnetic field in binary systems containing weakly magnetic neutron stars. We describe various processes by which the accretion disk interacts with the stellar magnetic field, the generation of toroidal magnetic fields in the magnetosphere, and termination of the Keplerian disk flow by the interaction.

In §3 we describe recent work on a unified model of the X-ray spectral states and quasi-periodic intensity oscillations (QPOs) of LMXBs. In this model, interaction of the disk with the small magnetosphere produces a hot central corona around the magnetosphere. When the luminosity approaches the Eddington critical luminosity, a cooler, more extensive corona forms above the inner part of the disk, and the neutron star begins to accrete matter from this corona as well as from the disk itself. Interaction of the photons from the neutron star with the inflow from the corona shapes the X-ray spectrum and can produce quasi-periodic intensity oscillations.

Finally, in §4 we describe several mechanisms that may accelerate particles to GeV or even TeV energies within the magnetosphere. These mechanisms include

acceleration by electric fields produced by interruption of field-aligned currents within the magnetosphere, formation of double layers, and release of stored magnetic energy via reconnection. Interaction of the resulting energetic charged particles with accreting matter may produce GeV or even TeV γ-radiation.

2. DISK-MAGNETOSPHERE INTERACTION

The interaction between the plasma in the accretion disk and the stellar magnetic field involves a variety of physical processes. We first describe current models of the inner part of geometrically-thin accretion disks and then discuss some of the physical processes by which the plasma in the inner part of the disk may interact with the stellar magnetic field. Next, we describe how these processes have been incorporated into a quasi-steady accretion flow model. Finally, we summarize the results of recent work on disk accretion by weakly magnetic neutron stars.

2.1 The Inner Part of Accretion Disks

The standard α-model of geometrically-thin, optically-thick accretion disks (62,63) divides naturally into three distinct parts: an "outer" part, where gas pressure exceeds radiation pressure and free-free absorption is more important than scattering; a "middle" part, where gas pressure exceeds radiation pressure but electron scattering is the dominant source of opacity; and an "inner" part, where electron scattering is the dominant opacity source and radiation pressure exceeds the gas pressure.

The structure and stability of the outer and middle parts of the α-disk are comparatively well understood. Cooling is efficient in these parts, and the disk is therefore quite thin ($h/r \sim 10^{-2}$–10^{-3}). The structure of the inner, radiation-pressure-dominated (RPD) part of the α-disk is much less clear. In particular, models of the RPD region that are optically thick in the vertical direction are thermally and viscously unstable if the shear stress is, as originally assumed, proportional to the *total* pressure (57,43,56,64,54). Because these models are unstable, alternative models of the inner part of the disk have been explored.

One of the first alternative models to be studied is the so-called β-model proposed by Cunningham (10), which assumes that the shear stress in the RPD region is proportional to the gas pressure alone. This model is both thermally and viscously stable. However, whether the shear stress can be proportional to the gas pressure in the RPD region remains uncertain, although it has been argued (72) that the shear stress produced by small-scale magnetic fields in the disk is proportional to the gas pressure, rather than the total pressure. Models in which the shear stress is proportional to the product of various fractional powers of the gas pressure and the total pressure have also been investigated (74,75).

An alternative approach has been to construct models of the inner disk that are *optically thin* in the vertical direction, in contrast to the models just described. Optically-thin models are much hotter than their optically-thick counterparts. As a result, gas pressure dominates radiation pressure. Also, the ions are typically much hotter than the electrons. Examples of such "two-temperature" disk models include the model proposed by Shapiro, Lightman, and Eardley (65), in which the electrons are cooled by Comptonization of an external source of soft photons, and so-called "Comptonized bremsstrahlung

Table 2.1 Models of the Inner Region of Accretion Disks

Disk Model	Thermal Modes	Viscous Modes
1T Opt thick GPD, shear stress $\propto P_{\rm tot}$	Stable	Stable
1T Opt thick RPD, shear stress $\propto P_{\rm tot}$	Unstable	Unstable
1T Opt thick RPD, shear stress $\propto P_{\rm gas}$	Stable	Stable
2T Opt thin GPD, Compt soft photons	Stable?[a]	Stable
2T Opt thin GPD, Compt brems	Stable?[a]	Stable

[a]The stability properties of these models are not yet certain (42,56,84,85).

models" (84,85), in which the dominant cooling mechanism is emission of bremsstrahlung which at high accretion rates is Comptonized by the electrons in the disk. In these models, the α prescription for the shear stress has generally been retained. In recent years, the effects of electron-positron pairs on such hot disk models have also been considered (41,30–32,76,84,85,6,7). Some essential features of the disk models described in this section are summarized in Table 2.1.

2.2 Physical Processes

Consider now the physical processes that create a couple between the disk flow and the neutron star. Near the inner edge of the Keplerian flow, the interface between the disk plasma and the magnetospheric plasma is Kelvin-Helmholtz unstable, as shown by Ghosh and Lamb (14–16; hereafter referred to as GL). Penetration of the Keplerian flow by the stellar magnetic field is assured if unstable modes grow to an amplitude comparable to the semi-thickness h of the disk. Modes with wavelengths λ greater than h can achieve such an amplitude while still in the linear regime. Since the growth times of the Kelvin-Helmholtz modes in the linear regime can be estimated analytically, using the MHD dispersion relation appropriate to the disk-magnetosphere interface, GL concentrated on long-wavelength modes. They found that near the inner edge of the disk, the growth time for long-wavelength Kelvin-Helmholtz modes is $\sim 10^{-5}$ times the radial drift time. Thus, there appears to be plenty of time for these modes to grow to sufficiently large amplitude to greatly disturb the disk surface and allow the magnetospheric magnetic field to mix with the disk plasma before the plasma drifts significantly inward. This mixing couples the stellar magnetic field and the disk.

The disk and the star are also coupled by turbulent diffusion of the stellar magnetic field into the disk (GL). This process is important in the region where the kinetic energy density of convective or turbulent motions in the disk exceeds the energy density of the stellar magnetic field just outside the disk. In this region one expects the stellar magnetic field to be entrained by the convective motions and carried into the disk. In order to make an estimate of the efficiency of this process, GL adopted a mixing length approach, assuming a diffusion coefficient $\sim 0.1\, u_t \ell_t$, where u_t is the turbulent velocity and ℓ_t is the length scale of the largest eddies. They found that the stellar magnetic field would

diffuse through the disk in a fraction $\sim 10^{-3}$ of the radial drift time. Thus, there appears to be ample time for the magnetic field to diffuse into the disk. Once inside the disk, magnetic field lines that were formerly above the disk can reconnect to magnetic field lines that were formerly below the disk, creating an additional couple between the disk and the neutron star just outside the inner edge.

A third process that couples the disk and the star is reconnection of the stellar magnetic field to magnetic fields in the disk (GL). The shear flow in the disk amplifies and reconnects any seed field in the stream of plasma that feeds it, creating closed loops of magnetic flux within the disk. These flux loops are continually distorted by convection and turbulence within the disk, and subdivided by reconnection (see [72] and references therein). Even if there were no magnetic field threading the disk plasma initially, turbulent diffusion of the magnetospheric magnetic field into the disk would create such a field. Once there are magnetic flux loops within the disk, either because magnetic fields were present initially or because the stellar magnetic field earlier diffused into the disk, it is be energetically favorable for the stellar magnetic field to reconnect to the magnetic fields in the disk. GL estimated that the time scale for this to occur near the inner edge of the disk is $\sim 10^{-3}$ times the radial drift time. In the usual reconnection picture, almost all of the magnetic flux is conserved, but the topology is completely changed. As a result, field lines that initially formed closed loops in the disk now connect to the star, producing a couple between the disk and the star.

In summary, even if the Keplerian disk plasma is not initially coupled to the stellar magnetic field, a significant couple will develop in a time short compared to the radial drift time.

The difference in the angular velocities of the star and the disk generates enormous electromotive forces that can drive large electrical currents within the magnetosphere if there is even a small density of charged particles there. Due to the plentiful supply of accreting plasma, the magnetosphere is expected to be almost exactly electrically neutral, and hence the electrical currents driven by the electromotive forces are conduction currents. The resulting $\mathbf{j} \times \mathbf{B}$ forces act on the matter in the star, the magnetosphere, and the disk to reduce their relative motion. The character of this electrodynamic interaction depends on the distribution of electrical resistance along the current paths.

GL examined this question and found that the electrical conductivity along field lines in the magnetosphere is high whereas the cross-field conductivity is likely to be much lower. They therefore concluded that cross-field currents are more likely to flow in the disk and the star than in the magnetosphere. As a result, they arrived at a system of field-aligned currents similar to the polar-cap ionospheric current system that is thought to couple the rotation of Jupiter's ionosphere to its magnetospheric sheath (27,28).

The velocity and magnetic fields in the picture proposed by GL are shown in the top panel of Figure 2.1. The azimuthal motion of the disk plasma relative to the star twists the stellar magnetic field, generating a toroidal component. The resulting magnetic stress acts to synchronize the orbital motion of the disk plasma and the rotation of the star. In an analogous manner, the radial inward motion of the plasma pinches the stellar magnetic field inward, partially screening the stellar magnetic field from the disk.

An equivalent circuit with lumped circuit elements is shown in the bottom panel of Figure 2.1. The rotation of the neutron star and the orbital motion of the disk plasma through the magnetic field generate the electromotive forces

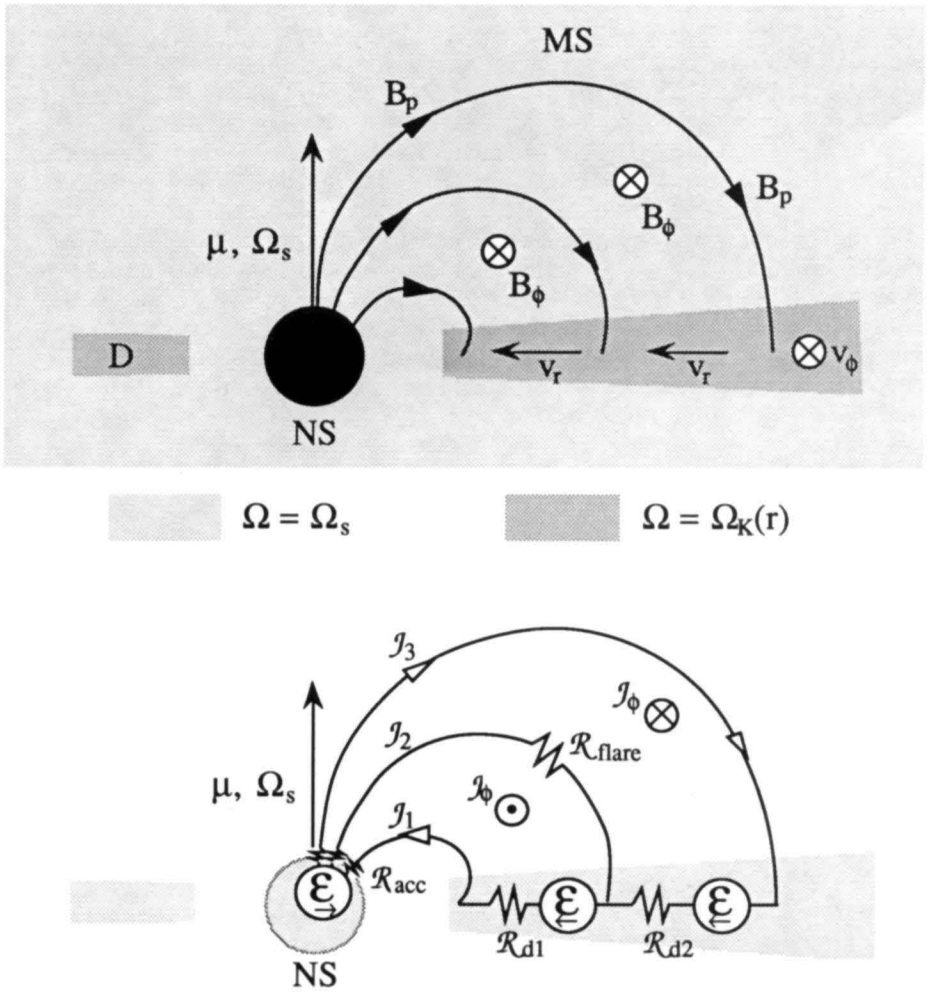

Fig. 2.1.—*Top*: Side view of a magnetic neutron star NS interacting with an acccretion disk D. Plasma in the lightly-shaded region corotates with the star, whereas plasma in the the heavily-shaded region circles the star in Keplerian orbits. *Bottom*: An equivalent circuit, showing the electromotive forces $\mathcal{E}$ produced by the rotation of the neutron star and the orbital motion of the disk plasma through the magnetic field, the resulting poloidal currents $\mathcal{J}_1$, $\mathcal{J}_2$, and $\mathcal{J}_3$, the corresponding azimuthal currents $\mathcal{J}_\phi$, and the circuit resistances $\mathcal{R}_{acc}$ in the accretion funnel and $\mathcal{R}_{d1}$ and $\mathcal{R}_{d2}$ in the disk. A steep rise in the resistance within the magnetosphere ($\mathcal{R}_{flare}$) will create a large potential drop. The resulting strong electric field can accelerate charged particles along the magnetic field.

labelled $\mathcal{E}$. These forces drive field-aligned currents within the highly-conducting magnetosphere, here represented by the poloidal currents $\mathcal{J}_1$, $\mathcal{J}_2$, and $\mathcal{J}_3$, and the azimuthal currents $\mathcal{J}_\phi$. The circuit is closed by cross-field currents flowing in the disk and the star. The flow of these currents through the resistances $\mathcal{R}_{\rm acc}$ in the accretion funnel and $\mathcal{R}_{\rm acc}$ and $\mathcal{R}_{\rm acc}$ in the disk produce potential drops that oppose the electromotive forces produced by the motion of the star and the disk plasma. Also important but not explicitly shown are the inductances of the current loops.

As the differential rotation of the disk plasma and star proceeds, the magnetic field linking them is increasingly twisted. The growing twist implies an ever increasing magnetic free energy and electrical current density within the magnetosphere. As GL emphasized, this increase in magnetic energy cannot continue indefinitely. Instead, the twisted and pinched magnetic field will relax. GL stressed relaxation via reconnection in the magnetosphere and via turbulent diffusion and reconnection in the disk.

Another possibility is that the high current density that develops in the magnetosphere due to the twisting of the field and pinch effects may drive the Bunemann or other microinstabilities. These instabilities are expected to develop when the electron-ion relative velocity exceeds the local sound speed (see [68]). They can greatly increasing the resistivity in a small region of the magnetosphere, interrupting the current and dissipating the magnetic energy.

Whatever the particular processes involved in a given system, the currents within the magnetosphere and the magnetic fields that they generate will be limited by instability. Depending on whether or not the dominant instability is self-adjusting, the free energy of the twisted magnetic field may be released fairly steadily, in freqent microflares, or in less frequent but much larger flares.

2.3 Steady Flow Models

GL emphasized that the magnetic free energy would almost surely be released in an episodic way. However, they also called attention to the difficulty of treating the release of this energy in any detailed way. They therefore suggested that, as a first step in understanding the large-scale behavior of disk-accreting neutron stars, it might be useful to attempt to describe the *time-averaged* properties of the magnetic field and the flow using a time-independent, non-ideal MHD model.

In order to proceed with this program, GL introduced an *effective* conductivity tensor $\sigma_{\rm eff}$ for the disk plasma, to describe the time-averaged effects of dissipative processes such as current-driven instabilities and reconnection. For simplicity, they assumed that $\sigma_{\rm eff}$ is isotropic and were then able to show that the value of $\sigma_{\rm eff}$ is determined by the assumption of a steady flow. They argued that magnetic field reconnection and other magnetic field dissipation processes are to some extent self-adjusting and therefore might maintain the time-averaged effective conductivity at this value. Using this approach, GL were able to develop a quantitative model of steady disk accretion by an aligned rotator by solving the 2D, non-ideal MHD equations in and near the disk plane and in the inner magnetosphere. GL emphasized that while time-independent solutions of the MHD equations may be useful for calculating average velocities, magnetic pitches, and the time-averaged accretion torque, time-dependent phenomena, such as flares, could also have observational consequences.

GL showed that the region where the stellar magnetic field threads the disk constitutes a *transition region* between undisturbed disk flow far from the star

and the flow inside the magnetosphere. The interaction between the *azimuthal* motion of the disk plasma in the transition region and the stellar magnetic field generates radial currents that tend to twist the field, as described above, creating an azimuthal field component. The interaction between the *radial* motion of the plasma in the transition region and the magnetic field generates azimuthal currents which tend to confine the poloidal field, creating a radial field component.

GL also showed that their 2D MHD model exhibits boundary layer behavior at the radius given implicitly by the angular momentum conservation condition

$$\frac{B_p B_\phi}{4\pi} 4\pi\varpi^2 \Delta\varpi \approx \dot{M}\varpi v_K \,, \tag{2.1}$$

that is, the velocity and magnetic fields in the model change on a length scale $\Delta\varpi \ll \varpi$ near the radius ϖ_0 given implicitly by equation (2.1). Thus, the transition region divides naturally into two zones: a broad outer zone, where the motion is Keplerian, and a narrrow inner zone, where the angular velocity falls sharply from the local Keplerian value to the stellar angular velocity at the radius ϖ_{co}. GL defined the radius ϖ_0 of the boundary between these two zones as the radius where $\partial\Omega/\partial\varpi = 0$. Thus, at $\varpi = \varpi_0$, the shear stress vanishes.

In the *inner transition zone*, between ϖ_{co} and ϖ_0, the interaction of the azimuthal flow with the magnetic field significantly reduces the angular velocity of the inflowing plasma from its Keplerian value just outside ϖ_0 to the corotational value at ϖ_{co}. In addition, azimuthal currents flowing in the disk plane and in the accreting plasma above and below the disk screen the poloidal component of the stellar magnetic field on the radial length scale

$$\Delta\varpi \approx \frac{c^2}{4\pi\sigma_{\rm eff} v_{\varpi 0}} \,, \tag{2.2}$$

where $v_{\varpi 0}$ is the radial velocity of plasma in the boundary layer. These screening currents reduce the poloidal field by a factor $\sim$5 between ϖ_{co} and ϖ_0.

In the *outer transition zone*, outside ϖ_0, the disk structure is similar to that of an undisturbed disk, except that angular momentum is removed from or fed into the disk by the stellar magnetic field, which is twisted by its interaction with the disk plasma. In addition, the total energy dissipation rate is augmented by resistive dissipation of the electrical currents flowing in the disk. GL found that the couple between the outer transition zone and the star is a substantial fraction of the total couple. Since the couple falls off gradually, the definition of the outer boundary of the outer transition zone is purely conventional.

The plasma in the disk is confined in the vertical direction by the pressure of the magnetospheric field rather than gravity inside a radius ϖ_p, which is somewhat larger than ϖ_0. Aly and Kuipers (2; see also ref. 29) have suggested that inside ϖ_p, plasma orbiting in the disk plane will break up into isolated clumps or blobs, which will then spiral inward due to their interaction with the stellar magnetic field. We emphasize that the time-averaged structure of this flow is necessarily similar to the structure in the same region of the quasi-steady GL model, and that the innermost radius at which the orbital motion of the blobs is Keplerian is, when calculated correctly, the same as the innermost radius of the Keplerian flow in the GL model.

2.4 The Inner Edge of the Disk

The radius ϖ_0 at which the Keplerian flow ends is an excellent diagnostic of conditions in the inner part of the disk, since it depends on the radial and vertical structure of this part, and directly affects several observable properties of accreting neutron stars, as well as their evolution (17).

The original work by GL concentrated on the strongly magnetic neutron stars that appear as accretion-powered pulsars. GL showed that the Keplerian flow in these systems is terminated by the stellar magnetic field in the middle part of the α disks. Subsequently, several developments have focused attention on disk accretion by weakly magnetic neutron stars. One was the discovery of weak-field millisecond pulsars and the proposal that they have been spun-up to millisecond periods by accretion from a disk while in a LMXB (see [5,71] and references therein). Another development was the discovery of high-frequency QPOs in the luminous LMXBs and the suggestion that these are caused by the interaction of a weak neutron star magnetic field with inhomogeneities in the inner part of the accretion disk (see §3).

In luminous LMXBs containing weakly magnetic neutron stars, the Keplerian disk flow is terminated by the stellar magnetic field in the inner part of the disk rather than in the middle part (83). However, the approach used by GL to determine the interaction of the stellar magnetic field with the middle disk is easily generalized to models of the inner disk (17). Whenever the Keplerian disk flow is terminated well within a given region of the disk, the innermost radius ϖ_0 of the Keplerian flow scales as particular fractional powers of the key accretion variables $\dot{M}$, μ, and M, that is

$$\varpi_0 \propto \dot{M}^a \mu^b M^c . \tag{2.3}$$

The values of the exponents a, b, and c depend on the particular model of the inner disk and boundary layer being considered. The values of these exponents are listed in Table 2.2 for the geometrically-thin α-disk models listed in Table 2.1

For Keplerian flows that end in the middle part of the disk, Table 2.2 lists the exact values of the exponents rather than the slightly different approximate values quoted in GL, to emphasize that the physical arguments used to derive the expression for ϖ_0 given in GL are fundamentally different from the physical arguments used to derive the expression for the radius of the magnetosphere in spherical accretion (40). Although these two expressions scale in almost the same way, the similarity of the scalings does *not* indicate that the basic physical processes are similar (35). This is a point on which there is considerable confusion in the literature.

Table 2.2 shows that when the Keplerian flow ends in the inner part of the disk, the scaling of ϖ_0 with the key accretion variables is generally quite different from the scaling when the Keplerian flow ends in the middle part of the disk. Moreover, different models of the inner disk produce quite different scalings of ϖ_0 with the key accretion variables. These scalings can be explored observationally in several ways (17). In particular, it may be possible to determine the scalings of the Keplerian frequency at ϖ_0 in different systems.

As one example, studies of the variation of the angular acceleration of accretion-powered pulsars with X-ray intensity can provide information on the scaling of the Keplerian frequency, and hence ϖ_0, with $\dot{M}$ (17). As another example, accurate measurements of the frequencies of the horizontal-branch

Table 2.2 Scaling of the Innermost Radius of the Disk

	$\varpi_0 \propto \dot{M}^a \mu^b M^c$		
Disk Model	Value of a	Value of b	Value of c
1T Opt thick GPD	−0.25	0.58	−0.21
1T Opt thick RPD*	−0.15	0.51	−0.13
2T Opt thin GPD Compt soft photon	−1.70	0.80	0.73
2T Opt thin GPD Compt brems	−0.48	0.57	0.05

*Scalings are the same for both prescriptions of the viscous shear stress listed in Table 2.1 (17), since the radius of the inner edge of the disk does not depend on the viscous shear stress (GL).

of QPOs—which are thought to reflect the difference between the stellar spin frequency and the Keplerian orbital frequency at ϖ_0 (see [38] and references therein)—may provide data on the variation of ϖ_0 with $\dot{M}$. Finally, studies of the so-called "spin-up line" for recycled pulsars in the P-$\dot{P}$ diagram—which is thought to reflect the Keplerian orbital frequency at ϖ_0 when the star is accreting at the Eddington critical rate $\dot{M}_E$ (see [77] and references therein)—may provide information on the scaling of ϖ_0 with μ. The details of these calculations and their implications are described elsewhere (17).

3. X-RAY SPECTRA AND QPOs

The unexpected discovery of quasi-periodic intensity oscillations (QPOs) in several LMXBs (80,44,23,52) has provided a wealth of information about these systems. By now, QPOs have now been detected in most of the luminous LMXBs.

Further clarity was achieved when it was realized that the spectral and temporal properties of the luminous LMXBs are closely correlated (55,79,19–22,33,24,26). In fact, recent studies (20–22,24,61,25,26) have shown that many of the most luminous LMXBs have three distinct spectral states, called the horizontal, normal, and flaring branches.

In the present section we described recent efforts to develop a unified model of the luminous LMXBs that can account for their X-ray spectral states and QPOs in a physically consistent way, emphasizing the physics of the accretion flow and the origin of the normal branch intensity oscillations. More detailed accounts of the model, including other aspects, may be found elsewhere (34–38,45,53,11–13,46,47).

3.1 Overview of the Unified Model

The unified model assumes that the X-ray source is a neutron star with a relatively weak ($B \sim 10^8$–10^9 G) magnetic field accreting matter from a disk fed by the companion star. The disk is disrupted by the magnetic field of the neutron star at ~15–20 km. The energy to power the X-ray emission comes

from release of the gravitational potential energy of the accreting matter as it approaches the neutron star. Most of the photons emitted by the source are produced in the inner disk and in a small central corona surrounding the neutron star magnetosphere.

When the luminosity is moderate, the optical depth of the inner disk corona and radial inflow is low and has only a small effect on the spectral and temporal properties of the emerging radiation. However, when the luminosity is within ~10% of the Eddington critical luminosity L_E, the outward force of the escaping radiation slows the radial inflow, the scattering optical depth of the inflow becomes ~5–15, and the inflow substantially alters the X-ray spectrum.

The ~20–50 Hz quasi-periodic oscillations observed primarily in the horizontal branch spectral state are assumed to be luminosity oscillations caused by interaction of the neutron star magnetosphere with the inner accretion disk (the magnetospheric beat-frequency modulated-accretion model; see [1,66]). The ~5–10 Hz quasi-periodic intensity oscillations observed in the normal branch spectral state are attributed to optical depth oscillations caused by interaction of escaping radiation with the radial inflow from the corona above the inner disk when the luminosity rises to within ~10% of L_E, as discussed below. The ~10–20 Hz quasi-periodic intensity oscillations observed in the flaring branch spectral state are attributed to photohydrodynamic modes that are excited by the oscillations in the radial flow and grow when the luminosity equals or exceeds the Eddington luminosity.

According to this model, the X-ray spectrum of LMXBs is formed in three physically distinct regions: (1) relatively cool ($T_e \sim 1$ keV), dense plasma near the neutron star, where comptonization is partially or fully saturated; (2) hotter ($T_e \sim$ 10–30 keV), less dense plasma in the inner disk and central corona, where comptonization is unsaturated; and, when the luminosity approaches and exceeds L_E, (3) a relatively cool ($T_e \sim 1$ keV) inner disk corona and radial flow, which partially degrades the radiation produced near the star. The sequence of horizontal, normal, and flaring branch spectral states observed in the Z-class sources is produced by the changing contributions of all three regions, as the mass accretion rate increases (34,36–38,46,47).

3.2 Accretion Flow

The inner disk probably consists of dense clumps of cooler plasma in Keplerian orbit, surrounded by a hot-proton plasma, as shown schematically in Figure 3.1. Protons in the hot plasma are heated by viscous energy dissipation and interaction with the magnetosphere and neutron star, and cooled by collisions with electrons. The resulting proton temperature in the hot plasma is ~100 MeV. The electrons in this plasma are heated by collisions with the protons and cooled by interaction with the ~1 keV radiation coming from the neutron star and magnetosphere. As a result, the electron temperature is ~10–20 keV.

The neutron star magnetosphere is filled with inflowing plasma, which is slowed by the outward force of radiation coming from near the star. Because of the high plasma density, the X-ray photosphere is some distance above the neutron star surface. Radiation produced in this region has a thermal spectrum with a characteristic temperature comparable to the effective temperature (~1 keV). High-harmonic cyclotron emission in the outer magnetosphere produces a substantial flux of soft photons.

The accretion flow pattern depends on the luminosity. At moderate luminosities (~0.5–0.9 L_E), the outward momentum of the radiation escaping from the

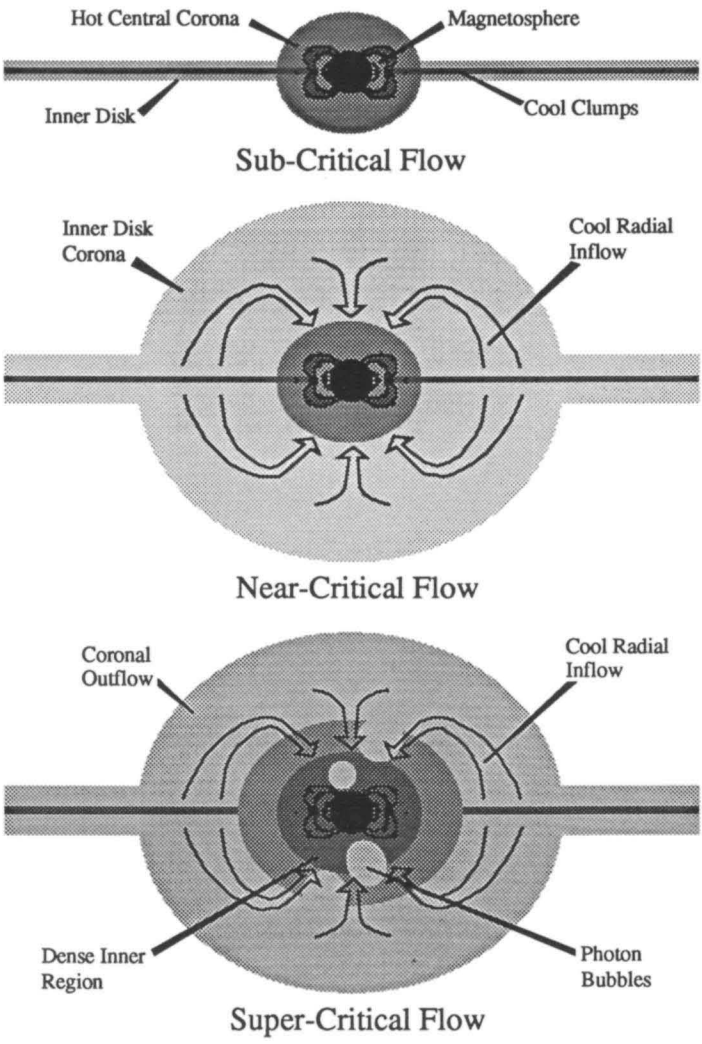

Fig. 3.1.—Schematic side views of the accretion flows discussed in the text. At moderate luminosities (top), the inner accretion disk consists of clumps of cooler plasma in Keplerian orbit, surrounded by a hot-proton plasma. Radiation forces cause the disk to thicken around the small neutron star magnetosphere, creating a compact central corona. At higher luminosities (middle), the inner disk expands vertically, forming a cool inner disk corona surrounding the hot central corona. The neutron star then accretes plasma from the inner disk corona as well as the disk (arrows). At luminosities above the Eddington limit, the radial flow near the central corona becomes unstable to growth of photohydrodynamic modes, which segregate the accreting plasma and outflowing radiation (bottom), allowing accretion to continue. After Lamb (36–38).

inner disk and neutron star causes the inner disk to thicken, forming a hot *central corona* around the small (radius ~15–20 km) magnetosphere of the neutron star, as shown schematically in the top panel of Figure 3.1. The electron scattering optical depth of the central corona is probably ~5. The radiation that emerges from the inner disk and central corona has a spectrum that is produced largely by unsaturated comptonization and therefore has a cutoff energy ~10–20 keV (36–38).

At luminosities $\gtrsim 0.9\,L_E$, the pressure of radiation escaping from the inner disk drives some plasma into a more extensive *inner disk corona* surrounding the central corona, as shown in the middle panel of Figure 3.1. Radiation drag causes plasma in the inner disk corona near the neutron star to lose its angular and vertical momentum and to fall approximately radially toward the star (11,12,37,38).

The size of the radiation drag and the structure of the radial flow depend on the mass flux $\dot{M}_d$ through the disk and the mass flux $\dot{M}_r$ in the radial flow. These are conveniently specified by the dimensionless parameters $\mu_d \equiv \dot{M}_d/\dot{M}_E$ and $\mu_r \equiv \dot{M}_r/\dot{M}_E$, where $\dot{M}_E$ is the mass flux that produces an accretion luminosity L_E. The total mass flux is then specified by the dimensionless parameter $\epsilon \equiv 1 - \mu_d - \mu_r$. Since $L_\infty/L_E \approx 1 - \epsilon$, the parameter ϵ is also a measure of the relative importance of the radiation force acting on the flow. Only two of the three parameters μ_r, μ_d, and ϵ are independent. When there is an adequate supply of matter, one expects $L_\infty \approx L_E$, and hence $\epsilon \ll 1$.

Inside the radius $r_{\rm radial} \approx 2\pi(1-\epsilon)^2 r_2$, where $r_2 \equiv GM/\epsilon c^2$, radiation drag removes the vertical and angular momentum of plasma orbiting in the inner disk corona in less than one Kepler period (11–13, 37,38). However, angular momentum conservation limits the radial mass flux to $\mu_r \leq \phi_s/c^2$, where ϕ_s is the gravitational potential at the neutron star surface (11,12,37,38). Thus, at most ~30% of the total mass flux onto the neutron star may come from the inner disk corona. If the inner disk corona is sufficiently dense, the actual radial mass flux should be near this maximum. Since the maximum is proportional to the luminosity, the radial mass flux may be approximately constant for luminosities near L_E.

Plasma in the inner disk corona that has lost angular momentum accelerates inward until its radial velocity reaches the value $\epsilon c/2$ at which the comoving luminosity equals L_E and the acceleration vanishes (45). Inside the inner critical radius $r_1 \equiv (\mu_r/\epsilon)R$ the flow becomes optically thick, radiation trapping is small but significant, and the flow velocity decreases linearly with radius (45) until gas pressure gradients become important (11–13). The time t_f required for gas captured from the inner disk corona to reach the neutron star is dominated by the inflow time from the outer part of the radial flow.

When the luminosity is $\gtrsim L_E$, nonaxisymmetric photohydrodynamic modes (69,70,18,81) develop in the slow radial flow near the neutron star magnetosphere (37,38,11). These modes may be metastable (69,70), requiring a finite-amplitude perturbation of the flow in order to grow. The normal branch oscillation of the radial flow provides such a perturbation, exciting photohydrodynamic modes of the same frequency (37,38,11). Growth of these modes segregates the accreting plasma and outflowing radiation as shown in the bottom panel of Figure 3.1, allowing the neutron star to continue to accrete even when its luminosity exceeds L_E. The optical depth oscillation produced by the dominant photohydrodynamic mode creates the X-ray intensity oscillation seen on the lower flaring branch (37,38,11).

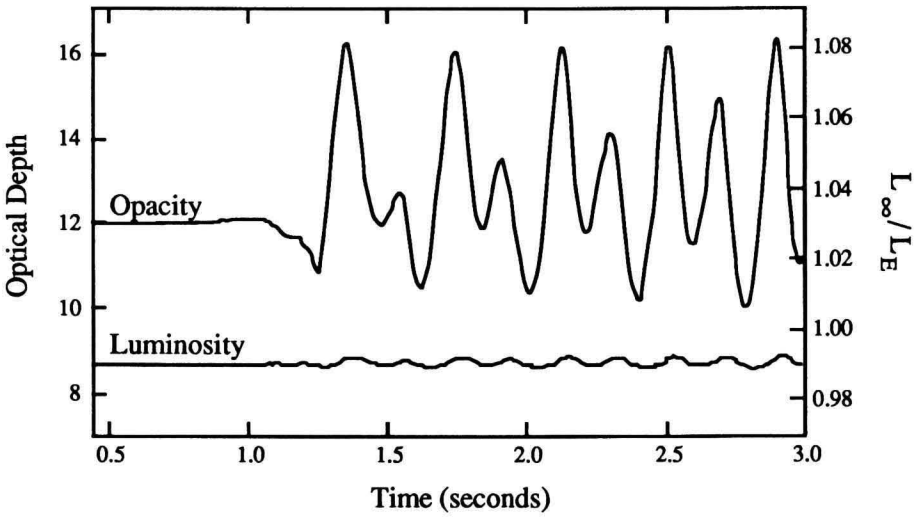

Fig. 3.2.—Variation of the electron scattering optical depth (left scale) and total luminosity (right scale) from a simulation of radial inflow from an inner disk corona. Note the stability of the flow before it was disturbed at 1.0 s, and the quasi-periodic oscillation that developed afterwards. The optical depth varies by ~30% whereas the luminosity varies by less than 1%. From ref. (11).

3.3 Normal Branch Oscillations

The accretion flow just described, which was originally developed to explain the X-ray spectral evolution on the normal branch, also provides a natural explanation of the NBOs (34–38,11–13). The reason is that the radial flow is very sensitive to perturbations in the mass flux and luminosity, when the luminosity is within ~10% of L_E. This sensitivity, and the unavoidable time lag between changes in the inward mass flux from the corona and the resulting luminosity changes, causes the radial flow to become overstable for luminosities sufficiently close to L_E.

This overstability has been demonstrated by an extensive study of the radial inflow of plasma from the inner disk corona, using a one-dimensional, time-dependent radiation hydrocode (11–13). In this study, steady, near-critical radial flows were first constructed. The stability of these flows was then investigated by disturbing the luminosity of the central corona or the inward mass flux from the outer boundary of the radial flow. The response of steady flows to perturbations of the luminosity or the mass flux was found to be very similar. When the luminosity is within ~10% of L_E and the fraction of the total mass flux in the radial flow is sufficiently high, both types of perturbations cause the radial flow to develop quasi-periodic oscillations.

Figure 3.2 shows results from an early simulation in which regular oscillations developed. For this particular run, $\mu_r = 0.05$ and $\epsilon = 0.01$. Similar results were obtained for ϵ values as large as 0.10. The inflow time t_f from the outer edge was ~0.3 s and the simulation was followed for ~10 inflow times.

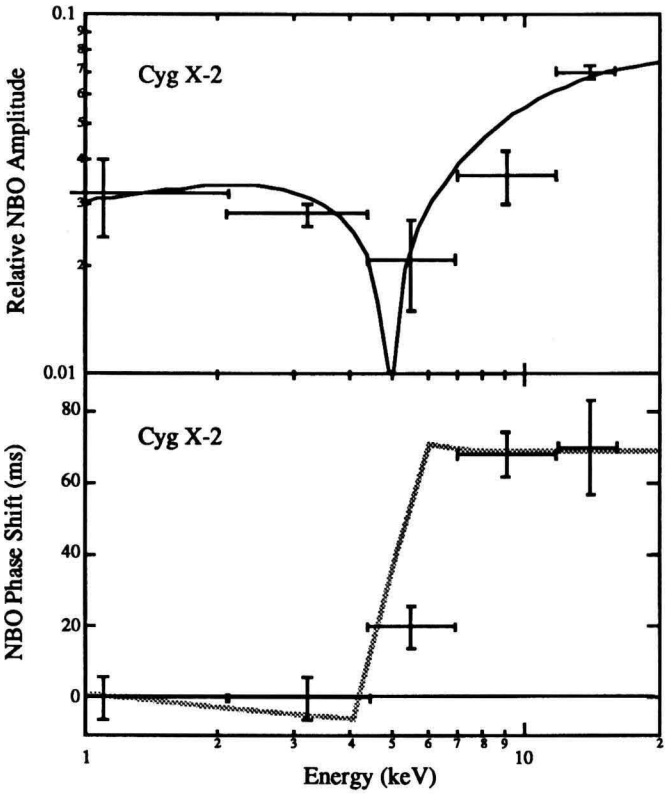

Fig. 3.3.—Observed (51) and calculated (47) Cyg X-2 normal branch oscillation amplitude (top) and phase (bottom), as a function of X-ray energy. The amplitude calculation assumes an optical depth of 10, an optical depth oscillation of 2, and an electron temperature of 0.8 keV.

The simulations that exhibited regular oscillations all had oscillation frequencies $f_{osc} \sim$ 5–10 Hz. These frequencies are comparable to the observed frequencies of NBOs at their onset near the middle of the normal branch. The scattering optical depths of the inflows that exhibited regular oscillations were all $\sim$10.

The relative amplitude $\Delta L/L$ of the luminosity oscillations tends to be much smaller than the relative amplitude $\Delta\tau_{es}/\tau_{es}$ of the oscillations in the scattering optical depth. This is to be expected, since the luminosity cannot vary by an amount greater than $\sim\epsilon L$ without disrupting the flow, whereas variations in the luminosity of this magnitude produce large variations in the density and optical depth of the flow. Thus, these simulations support the earlier suggestion (34,36–38) that NBOs are primarily oscillations in optical depth rather than luminosity.

Numerical calculations of the effect of optical depth oscillations on the X-ray spectrum (47) show that such oscillations cause the spectrum to rotate about a pivot energy E_p that depends on the spectrum, but is in the range 2–7 keV for observed spectra. The quasi-periodic oscillations in the optical depth of the radial flow therefore cause the X-ray spectrum to rock quasi-periodically about the energy E_p, in effect moving the source a small distance up and down the normal branch. A byproduct of this motion is that the X-ray intensity oscillates quasi-periodically in most energy bands.

These predictions agree quantitatively with the properties of the NBO in Cyg X-2, as shown in Figure 3.3. The amplitude minimum at $\sim$5 keV indicates that the electron temperature in the radial flow is $\sim$0.8 keV. The $\sim$150°. phase *lag* of the NBOs above E_s relative to the NBOs below E_s reported by Mitsuda (48,49) and Mitsuda and Dotani (51) is, in this model, actually a $\sim$210° phase *lead*, composed of the 180° phase lead produced by the rocking of the spectrum, plus an additional $\sim$20° phase lead (equivalent to $\sim$10 ms) due to the time required for photons to downscatter to energies less than E_s. These predictions also agree quantitatively with observations of GX 5−1, which has a normal branch pivot energy $\sim$2 keV (Hasinger, personal communication) and a minimum in the NBO amplitude at about the same energy (50).

4. PARTICLE ACCELERATION

The outer magnetosphere of an accreting neutron star, where the magnetic field of the star interacts strongly with a relatively dense plasma flow, is a natural site for acceleration of charged particles by a variety of mechanisms. Moreover, the presence of a strong magnetic field and accreting plasma may allow the energy of accelerated particles to be converted efficiently into γ-rays. Processes that may produce a substantial luminosity of MeV γ-rays are of special current interest, since the *Gamma-Ray Observatory* is scheduled for launch in the near future. In addition, there have been numerous reports of occasional detection of much higher-energy radiation from accretion-powered neutron stars, including radiation at TeV and even PeV energies.

In this section we summarize the basic features of the TeV radiation reported from neutron stars and indicate some of the constraints on models of TeV emission imposed by these reports. We then suggest that magnetospheric flares may be an important source of high-energy photons.

4.1 Observational Requirements

Detection of occasional TeV and even PeV radiation has been reported from about a dozen accretion-powered neutron stars, including Her X-1, and from about half a dozen rotation-powered neutron stars, including the Crab pulsar (8,82). In many cases, the reported detections have not yet been confirmed. The duty cycles of the emission appear to be quite small ($\lesssim 10^{-2}$). Moreover, there are indications that the radiation reported at PeV energies does not have the signature of γ-rays (9). Nevertheless, there are enough confirmed reports of TeV radiation from neutron stars that it seems worthwhile to consider what processes might produce such energetic radiation. Models of TeV γ-radiation from rotation-powered pulsars have been reviewed extensively by Ruderman (58,59). Here we restrict our discussion to models of TeV γ-ray emission from accretion-powered neutron stars.

The main arguments for interpreting the reported TeV radiation from neutron stars as γ-rays have been summarized by Ruderman (59). In order for the radiation to preserve an intensity oscillation with a period close to the neutron star spin period ($\sim$seconds) even after flight times much greater than 10^4 years, as claimed, and to arrive from the direction of the neutron star, the radiation must be neutral, almost massless relative to its energy, and able to penetrate at least $10^{-2}\,\mathrm{g\,cm^{-2}}$ of interstellar matter without degradation. Among known

particles, only photons and neutrinos meet these requirments, but TeV neutrinos would not cause the reported air showers.

Any mechanism for producing the presumed TeV γ-radiation from accreting neutron stars must meet the following basic observational requirements:

- It must be capable of producing γ-rays with energies of 10^{12} eV or higher.
- It must be capable of producing a γ-ray luminosity at least $\sim 10^{-2}$ times the X-ray luminosity of accretion-powered pulsars.
- It should account for the episodic character of the emission, which sometimes lasts $\sim 10^3$ s, and be compatible with the low observed duty cycles of the radiation ($\sim 10^{-2}$ to $\sim 10^{-7}$).
- It should explain the periodicity of the γ-ray emission in accretion-powered pulsars, which is reportedly close to but not exactly equal to the X-ray period, with typical differences of about 1 part in 10^3.
- If the radiation is beamed, it should be beamed in the disk plane, at least in Her X-1 and Vela X-1, since the TeV radiation reported from Her X-1 varies in phase with the 35-day cycle while the TeV radiation reported from Vela X-1 appears to be eclipsed by the neutron star's companion.

The above observational requirements impose strong constraints on models of the emission.

4.2 Theoretical Constraints

In order to produce TeV γ-rays, it is likely that charged particles must be accelerated to even higher energies. Several theoretical considerations are relevant to such models:

- Near accreting neutron stars, acceleration of electrons to energies as high as 10^{12}–10^{13} eV may sometimes, though not always, be prevented by the drag force produced by inverse Compton scattering of X-rays coming from the star. For this reason, most workers have focused on acceleration of protons.
- Proton acceleration cannot occur too far from the star, since the total luminosity available at the radius $R_{\rm acc}$ at which particle acceleration occurs is unlikely to exceed $(R/R_{\rm acc})\,L_x$, where L_x is the X-ray luminosity.
- The acceleration process must be consistent with the known environments of neutron stars. For example, observations indicate that the plasma particle density at 10^8–10^9 cm from the neutron star in Her X-1 is $\gtrsim 10^{12}\,{\rm cm}^{-3}$ (3,4).
- If protons are accelerated by an electric field, the acceleration must be parallel to the magnetic field, since the proton gyroradius is typically small compared to the acceleration length. Electric fields that exceed the magnetic field ($E > B$), allowing protons to move across magnetic field lines, are likely only in regions that are small compared to the acceleration length.
- Protons that have been accelerated to $\sim 10^{13}$ eV can convert their energy fairly efficiently to TeV γ-rays, if they traverse a plasma target of appropriate thickness. According to Stenger (73), the optimal column density for the target is $\sim 50\,{\rm g\,cm}^{-2}$. For such a target, each proton will produce about five γ-rays, each having an energy $\sim 3\%$ of the initial proton energy (see [67]). Since the absorption length for such γ-rays is $\sim 75\,{\rm g\,cm}^{-2}$, few are absorbed in the target.
- Production of TeV γ-radiation must occur sufficiently far from the neutron star that the magnetic field strength is less than 10^6 G; otherwise such

energetic γ-rays will be converted to electron-positron pairs after traveling only a short distance.

One process that may meet these requirements is electrodynamic acceleration of protons in the outer magnetosphere, above and below the inner edge of an accretion disk.

4.3 Magnetospheric Acceleration

The interaction of the disk with the stellar magnetic field described in §.2 suggests several scenarios for accelerating charged particles in the outer magnetosphere. Here we briefly discuss three possibilities. Particle acceleration in the outer magnetosphere and associated production of γ-rays is discussed in more detail by Lamb *et al.* (39).

Consider again the picture of the velocity and magnetic fields shown in the top panel of Figure 2.1. Twisting of the stellar magnetic field causes the magnetosphere to balloon outward. At the same time, a localized region of high azimuthal magnetic pitch develops above and below the disk plane (86,87,35). This region of high pitch produces a region of high azimuthal current density. If the current density becomes sufficiently large, current-driven instabilities will produce an anomalously high resistivity in this region (see [68]). Depending on whether or not the instability is self-adjusting, the free energy of the twisted magnetic field may be released fairly steadily or in a large flare. While the resistance is high, a large potential drop will develop across the resistive region. The resulting strong electromotive force

$$\mathcal{E}_{\rm tot} \approx \mathcal{E}_{\rm disk} - \mathcal{E}_{\rm star} \approx \frac{1}{c}(\Omega_{K0} - \Omega_s)B_0 r_0^2 \sim 10^{15} \ \text{Volts} \qquad (4.1)$$

may accelerate charged particles along the magnetic field. The time development of such a circuit can often be described by equivalent circuits with lumped circuit elements, like those shown in the bottom panel of Figure 2.1.

A second possibility is that double layers may develop within the magnetosphere (again see [68]). Such laminar space-charge layers trap a large fraction of the current-carrying electron population and accelerate the remainder. They can accelerate particles to high energies and can be modeled by an equivalent circuit having a capacitor and a resistor parallel to the magnetic field lines; however, the capacitance and resistance must be treated as highly nonlinear functions of the electric field in the layer.

A third possibility is that the energy stored in the twisted stellar magnetic field is released by reconnection, as suggested by GL. In fast rotators, the azimuthal field reverses sign at $r_c \approx r_0$. The resulting current sheet may tear, releasing the stored magnetic energy. Reconnection near the inner edge of the disk has recently been discussed in more detail by Aly and Kuipers (2) and Kuipers (29).

Figure 4.1 shows a possible scenario for producing energetic γ-rays with the right beam direction by accelerating protons in a resistive region, double layer, or reconnection zone within the magnetosphere. The protons enter the disk at an oblique angle where the highly twisted magnetic field from the acceleration region threads the disk. Collisons of the energetic protons with protons in the disk produce π_0's which then decay, generating a beam of γ-rays close to the disk plane. If the acceleration is electrodynamic, only those stars with $\boldsymbol{\mu} \cdot \boldsymbol{\Omega}_s > 0$

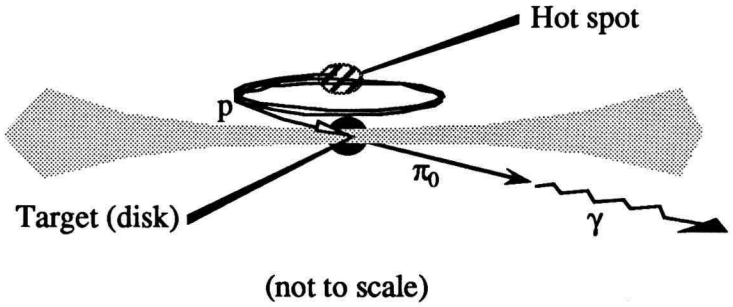

Fig. 4.1.—Perspective schematic view of γ-ray production by a magnetic neutron star accreting from a disk. Protons are accelerated in a resistive region, double layer, or reconnection zone within the magnetosphere. They then enter the disk at an oblique angle where the highly twisted magnetic field from the acceleration region threads the disk. The accelerated protons collide with protons in the disk, producing energetic π_0's. When the π_0's decay, they generate a beam of γ-rays close to the disk plane.

can produce γ-rays in this way, since only such stars will accelerate protons toward the disk.

Because the potential drop across the acceleration region necessarily leads to differential rotation within the magnetosphere, we do not expect these mechanisms to produce γ-radiation that oscillates in intensity at *exactly* the stellar spin frequency. Indeed, unless the energy release is relatively steady and the magnetosphere is quiescent, the spread in pattern frequencies is likely to be comparable to the spread in the Keplerian frequencies of the disk plasma that is threaded by the magnetic flux from the acceleration region. However, the long-term average of the frequencies of any oscillations in the intensity of the γ-rays should be equal to the stellar spin frequency.

5. REFERENCES

1. Alpar, M. A., and Shaham, J. 1985, *Nature*, **316**, 239.
2. Aly, J.-J., and Kuipers, J. 1990, *Astron. Ap.*, **227**, 473.
3. Bai, T. 1980, *Astrophys. J.*, **239**, 334.
4. Becker, R. H., *et al.* 1977, *Astrophys. J.*, **214**, 879.
5. Bhattacharya, D., and van den Heuvel, E. P. J. 1991, *Phys. Rep.*, in press.
6. Björnsson, G. 1990, Ph.D. Thesis, University of Illinois at Urbana-Champaign.
7. Björnsson, G., and Svensson, R. 1991, *Astrophys. J.*, in press.
8. Chadwick, P. M., McComb, T. J. L., and Turver, K. E. 1990, *J. Phys. G*, **16**, 1773.
9. Cronin, J. 1990, in *Proc. XIV International Symposium on Lepton and Photon Interactions*, in press.
10. Cunningham, C. T. 1973, Ph.D. Thesis, University of Washington.
11. Fortner, B. F., Lamb, F. K., and Miller, G. S. 1989, *Nature*, **342**, 775.
12. Fortner, B. F., Lamb, F. K., and Miller, G. S. 1991a, *Ap. J.*, submitted.
13. Fortner, B. F., Lamb, F. K., and Miller, G. S. 1991b, in preparation.
14. Ghosh, P., and Lamb, F. K. 1978, *Astrophys. J.*, **223**, L83 (GL).
15. Ghosh, P., and Lamb, F. K. 1979, *Astrophys. J.*, **232**, 259 (GL).
16. Ghosh, P., and Lamb, F. K. 1979, *Astrophys. J.*, **234**, 296 (GL).

17. Ghosh, P., and Lamb, F. K. 1991, in preparation.
18. Hameury, J. M., Bonazzola, S., and Heyvaerts, J. 1980, *Astron. Ap.*, **90**, 359.
19. Hasinger, G. 1987, in *IAU Symposium* **125**, *The Origin and Evolution of Neutron Stars*, ed. D. J. Helfand and J. H. Huang (Dordrecht: Reidel), p. 333.
20. Hasinger, G. 1987, *Astron. Ap.*, **186**, 153.
21. Hasinger, G. 1988, in *Physics of Compact Objects*, ed. N. E. White and L. G. Filipov (*Adv. Space Res.*, **8**), p. 377.
22. Hasinger, G. 1988, in *Physics of Neutron Stars and Black Holes*, ed. Y. Tanaka (Tokyo: Universal Academy), p. 97.
23. Hasinger, G., Langmeier, A., Sztajno, M., Trümper, J., Lewin, W.H.G., and White, N. E. 1986, *Nature*, **319**, 469.
24. Hasinger, G., Priedhorsky, W. C., and Middleditch, J. 1989, *Astrophys. J.*, **337**, 843.
25. Hasinger, G., and van der Klis, M. 1989, *Astron. Ap.*, **225**, 79.
26. Hasinger, G., van der Klis, M., Ebisawa, K., Dotani, T., and Mitsuda, K. 1990, *Astron. Ap.*, **235**, 131.
27. Kennel, C. F., and Coroniti, F. V. 1975, in *The Magnetospheres of the Earth and Jupiter*, ed. V. Formisano (Dordrecht: Reidel), p. 451.
28. Kennel, C. F., and Coroniti, F. V. 1977, *Ann. Rev. Astron. Astrophys.*, **15**, 389.
29. Kuipers, J. 1990, in *Active Close Binaries*, ed. C. Ibanoğlu and I. Yavuz (Dordrecht: Kluwer Academic Publ.), in press.
30. Kusunose, M., and Takahara, F. 1988, *Pub. Astr. Soc. Japan*, **40**, 435.
31. Kusunose, M., and Takahara, F. 1989, *Pub. Astr. Soc. Japan*, **41**, 263.
32. Kusunose, M., and Takahara, F. 1990, *Pub. Astron. Soc. Japan*, in press.
33. Lamb, F. K. 1988, in *Physics of Compact Objects*, ed. N. E. White and L. G. Filipov (*Adv. Space Res.*, **8**), p. 421.
34. Lamb, F. K. 1988, Talk presented at the Los Alamos Workshop on QPOs, La Cienega, N.M., September 1988.
35. Lamb, F. K. 1989, in *Timing Neutron Stars*, ed. H. Ögelman and E.P.J. van den Heuvel (Dordrecht: Kluwer), p. 649.
36. Lamb, F. K. 1989, in *Proc. 14th Texas Symp. on Relativistic Astrophysics*, ed. E. J. Fenyves (*Ann. NY Acad. Sci.*, **571**), p. 347.
37. Lamb, F. K. 1989, in *Proc. 23rd ESLAB Symp. on X-Ray Astronomy*, ed. N. E. White (ESA SP-296), p. 215.
38. Lamb, F. K. 1991, *Ap. J.*, in press.
39. Lamb, F. K., Ghosh, P., Hamilton, R., and Miller, M. C. 1991, in preparation.
40. Lamb, F. K., Pethick, C. J., and Pines, D. 1973, *Astrophys. J.*, **184**, 271.
41. Liang, E.P.T. 1979, *Astrophys. J.*, **234**, 1105.
42. Lightman, A. P. 1990, personal communication.
43. Lightman, A. P., and Eardley, D. M. 1974, *Astrophys. J. (Letters)*, **187**, L1.
44. Middleditch, J., and Priedhorsky, W. C. 1986, *Astrophys. J.*, **306**, 230.
45. Miller, G. S.1990, *Astrophys. J.*, **356**, 572.
46. Miller, G. S., and Lamb, F. K. 1988, Talk presented at the Los Alamos Workshop on QPOs, La Cienega, N.M., September 1988.
47. Miller, G. S., and Lamb, F. K. 1991, in preparation.
48. Mitsuda, K. 1988, in *Physics of Compact Objects*, ed. N. E. White and L. G. Filipov (*Adv. Space Res.*, **8**), p. 391.
49. Mitsuda, K. 1988, in *Physics of Neutron Stars and Black Holes*, ed. Y. Tanaka (Tokyo: Universal Academy), p. 117.

50. Mitsuda, K. 1989, in *Proc. 23rd ESLAB Symp. on X-Ray Astronomy*, ed. N. E. White (ESA SP-296), p. 197.
51. Mitsuda, K., and Dotani, T. 1989, *Pub. Astr. Soc. Japan*, **41**, 557.
52. Norris, J. P., and Wood, K. S. 1987, *Astrophys. J.*, **312**, 732.
53. Park, M.-G., and Miller, G. S. 1991, *Ap. J.*, in press.
54. Piran, T. 1978, *Astrophys. J.*, **221**, 652.
55. Priedhorsky, W. C., Hasinger, G., Lewin, W.H.G., Middleditch, J., Parmar, A., Stella, L., and White, N. 1986, *Astrophys. J. (Letters)*, **306**, L91.
56. Pringle, J. E. 1976, *Mon. Not. R. astr. Soc.*, **177**, 65.
57. Pringle, J. E., Rees, M. J., and Pacholczyk, A. G. 1973, *Astron. Ap.*, **29**, 179.
58. Ruderman, M. 1989, Talk presented at the NASA EGRET Symposium, Greenbelt, Maryland.
59. Ruderman, M. 1990, Proc. XIV International Symposium on Lepton and Photon Interactions, in press.
60. Schreier, E. J., *et al.* 1972, *Astrophys. J.*, **172**, L79.
61. Schulz, N. S., Hasinger, G., and Trümper, J. 1989, *Astron. Ap.*, **225**, 48.
62. Shakura, N. I. 1972, *Astron. Zh.*, **49**, 921 [Engl. transl. *Sov. Astron.–AJ*, **16**, 756].
63. Shakura, N. I., and Sunyaev, R. A. 1973, *Astron. Ap.*, **24**, 337.
64. Shakura, N. I., and Sunyaev, R. A. 1976, *Mon. Not. R. astr. Soc.*, **175**, 613.
65. Shapiro, S. L., Lightman, A. P., and Eardley. D., M. 1976, *Astrophys. J.*, **204**, 187.
66. Shibazaki, N., and Lamb, F. K. 1987, *Astrophys. J.*, **318**, 767.
67. Slane, P., and Fry, W. F. 1989, *Astrophys. J.*, **342**, 1129.
68. Spicer, D. S. 1982, *Space Sci. Rev.*, **31**, 351.
69. Spiegel, E. A. 1976, in *Physique des Mouvements dans les Atmosphères Stellaires* (Paris: CNRS), p. 19.
70. Spiegel, E. A. 1977, in *IAU Colloq.* **38**, *Problems of Stellar Convection*, ed. J. Ehlers, K. Hepp, R. Kippenhahn, H. A. Weidenmüller, and J. Zittartz (Berlin: Springer-Verlag), p. 19.
71. Srinivasan, G. 1989, *Astron. Ap. Rev.*, **1**, 209.
72. Stella, L., and Rosner, R. 1984, *Astrophys. J.*, **277**, 312.
73. Stenger, V. J. 1984, *Astrophys. J.*, **284**, 810.
74. Szuszkiewicz, E. 1990, *Mon. Not. R. astr. Soc.*, **244**, 377.
75. Taam, R. E., and Lin, D. N. C. 1984, *Astrophys. J.*, **287**, 761.
76. Tritz, B., and Tsuruta, S. 1989, *Astrophys. J.*, **340**, 203.
77. van den Heuvel, E.P.J. 1989, in *Timing Neutron Stars*, ed. H. Ögelman and E.P.J. van den Heuvel (Dordrecht: Kluwer Academic Publ.), p. 523.
78. van der Klis, M. 1989, *Ann. Rev. Astr. Ap.*, **27**, 517.
79. van der Klis, M., Jansen, F., van Paradijs, J., Lewin, W.H.G., Sztajno, M., and Trümper, J. 1987, *Astrophys. J. (Letters)*, **313**, L19.
80. van der Klis, M., Jansen, F., van Paradijs, J., Lewin, W.H.G., van den Heuvel, E.P.J., Trümper, J., and Sztajno, M. 1985, *Nature*, **316**, 225.
81. Wang, Y.-M. 1982, *Astron. Ap.*, **112**, 24.
82. Weekes, T. C. 1988, *Phys. Rep.*, **160**, 1.
83. White, N. E., and Stella, L. 1987, *Mon. Not. R. astr. Soc.*, **231**, 325.
84. White, T. R., and Lightman, A. P. 1989, *Astrophys. J.*, **340**, 1024.
85. White, T. R., and Lightman, A. P. 1990, *Astrophys. J.*, **352**, 495.
86. Zylstra, G. 1988, Ph.D. thesis, University of Illinois at Urbana-Champaign.
87. Zylstra, G., Lamb, F. K., and Aly, J.-J. 1991, in preparation.